Supporting Information for

Revisited Wurtzite CdSe Synthesis : a Gateway for the Versatile Flash Synthesis of Multi-Shell Quantum Dots and Rods

Emile Drijvers,[1,3] Jonathan De Roo,[2] Pieter Geiregat,[1,3] Krisztina Fehér,[4] Zeger Hens[1,3] and Tangi Aubert[1,3]

[1] Physics and Chemistry of Nanostructures (PCN), and [2] Sol-gel Centre for Research on Inorganic Powders and Thin films Synthesis (SCRiPTS), Department of Inorganic and Physical Chemistry, Ghent University, Krijgslaan 281-S3, 9000 Ghent, Belgium.

[3] Center for Nano and Biophotonics (NB-Photonics), Ghent University, Sint-Pietersnieuwstraat 41, 9000 Ghent, Belgium.

[4] NMR and Structure Analysis Unit, Department of Organic and Macromolecular Chemistry, Ghent University, Krijgslaan 281-S4, 9000 Ghent, Belgium.

Corresponding authors: Zeger.Hens@UGent.be, Tangi.Aubert@UGent.be

Content:

Section S1 :
Additional absorption and photoluminescent spectra, photoluminescent decays, table of optical properties and TEM images.

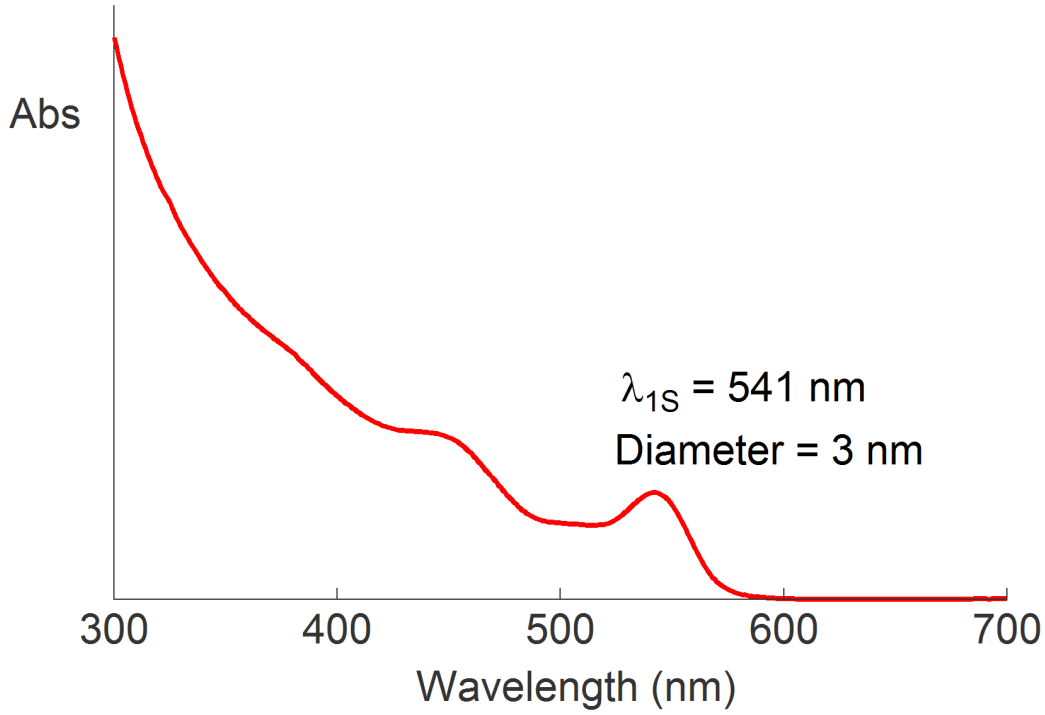

Figure S1. Absorption spectrum of a CdSe QDs sample used for subsequent shell growth.

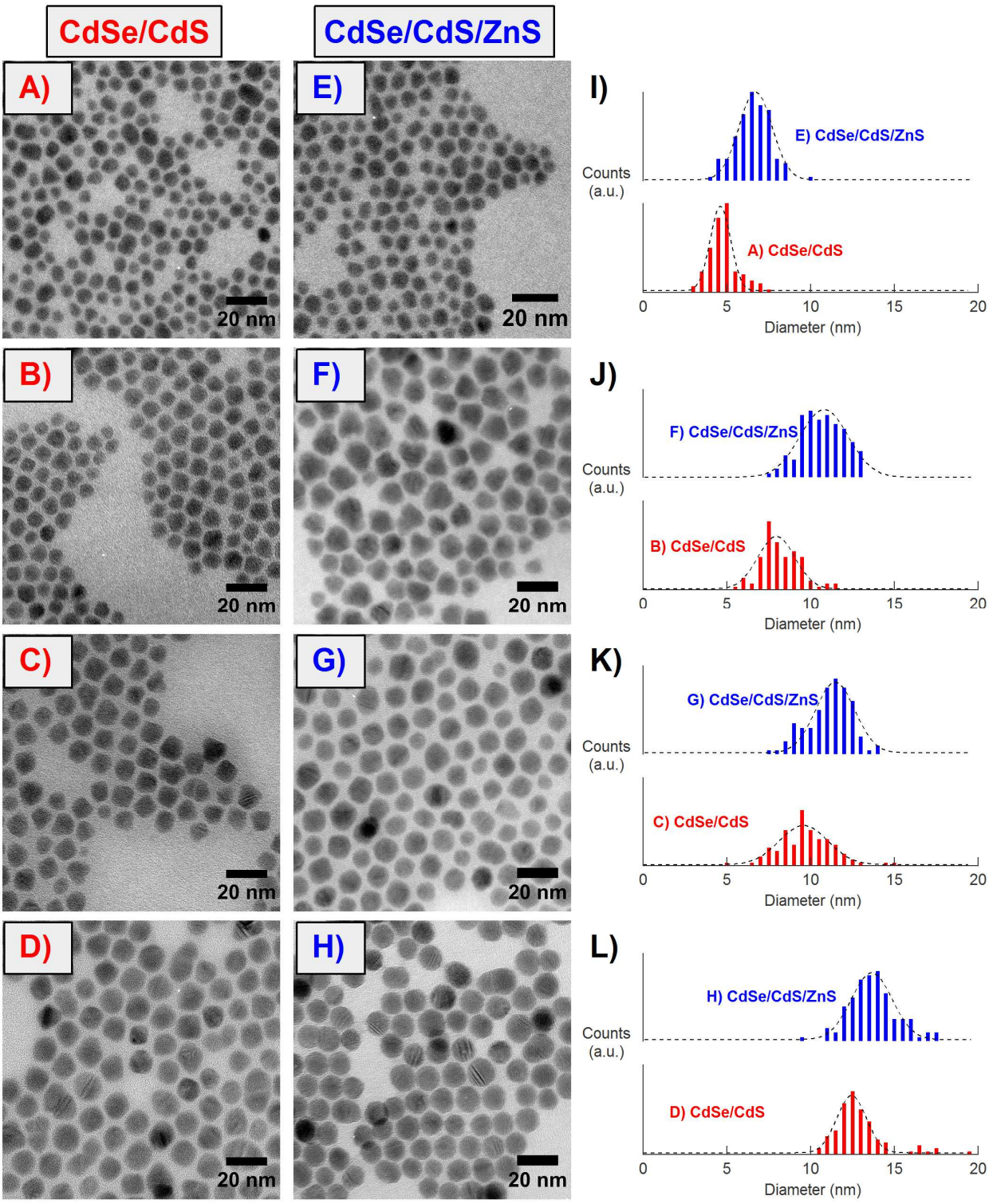

Figure S2. TEM images of a) CdSe/CdS QDs of 5.0 ± 0.9 nm, b) 8.5 ± 1.2 nm, c) 9.9 ± 1.6 nm and d) 13.4 ± 2.0 nm produced from the same 3 nm CdSe cores via the *flash* synthesis. TEM images of e) CdSe/CdS/ZnS QDs of 6.8 ± 1.0 nm, f) 10.9 ± 1.5 nm, g) 11.3 ± 1.3 nm and h) 14.0 ± 1.5 nm grown from a), b), c) and d) respectively. Histograms i), j), k) and l) show the size distributions of the CdSe/CdS and CdSe/CdS/ZnS QD samples. An overview of the optical properties of these particles can be found in **Table S1**.

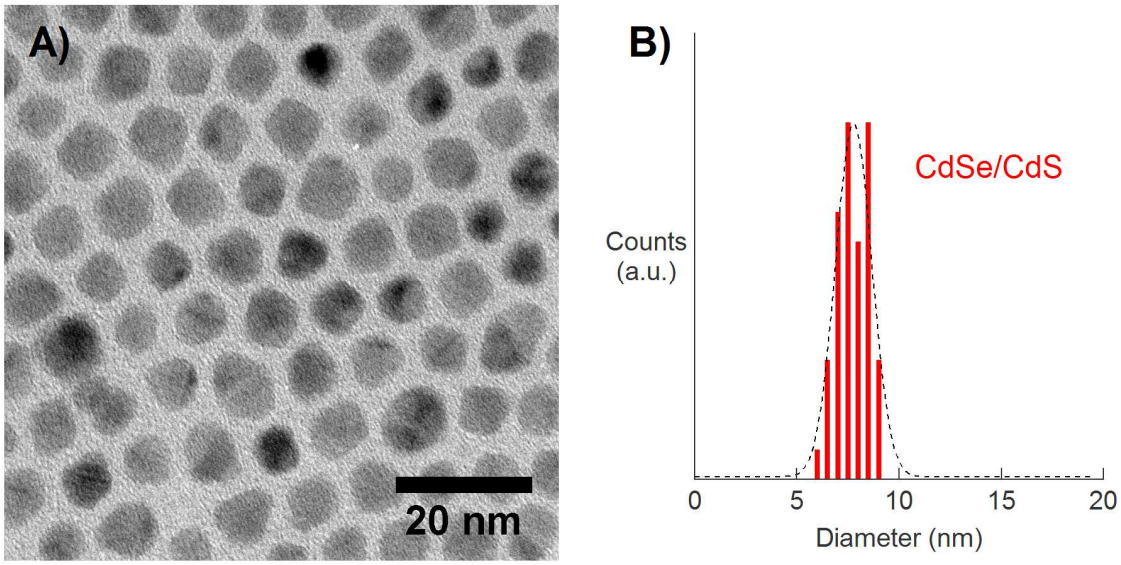

Figure S3. a) TEM image and b) histogram of core-shell CdSe/CdS QDs with size dispersions below 10% when increasing the concentration of the seeds from 200 nmol to 400 nmol in the *flash* synthesis.

Table S1. Overview of properties of core-shell QDs with different sizes. TEM images and size histograms of QDs A through H can be found in **Figure S2**

Sample	Seeds used	Composition	Diameter (nm)	ZnS thickness (nm)	Emission (nm)	PLQY (%)
A	3 nm CdSe	CdSe/CdS	5.0 ± 0.9	-	586	48 ± 2.1 %
E	A	CdSe/CdS/ZnS	6.8 ± 1.0	0.9	587	51 ± 2.5 %
B	3 nm CdSe	CdSe/CdS	8.5 ± 1.2	-	615	67 ± 1.7 %
F	B	CdSe/CdS/ZnS	10.9 ± 1.5	1.2	614	68 ± 2.2 %
C	3 nm CdSe	CdSe/CdS	9.9 ± 1.6	-	622	60 ± 1.5 %
G	C	CdSe/CdS/ZnS	11.3 ± 1.3	0.7	617	72 ± 2.8%
D	3 nm CdSe	CdSe/CdS	13.4 ± 2.0	-	622	36 ± 0.7 %
H	D	CdSe/CdS/ZnS	14.0 ± 1.5	0.3	620	47 ± 1.0 %

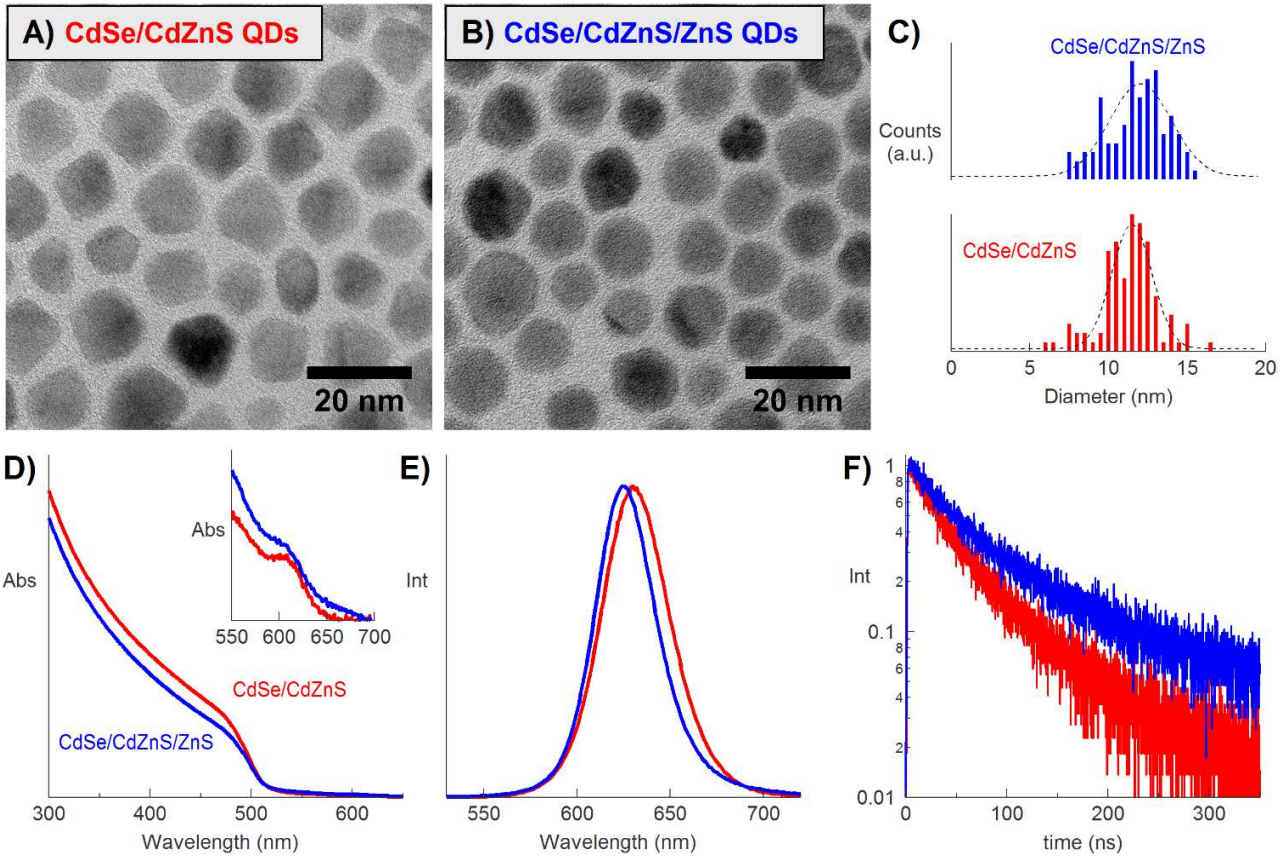

Figure S4. TEM images of a) CdSe/CdZnS and b) CdSe/CdZnS/ZnS QDs with c) histograms of the diameters measured from TEM images. Optical properties with d) absorption spectra normalized to QD concentration determined by ICP measurements (inset: focus on the excitonic feature at 600 nm), E) normalized emission spectra and f) normalized photoluminescence decays of the QDs.

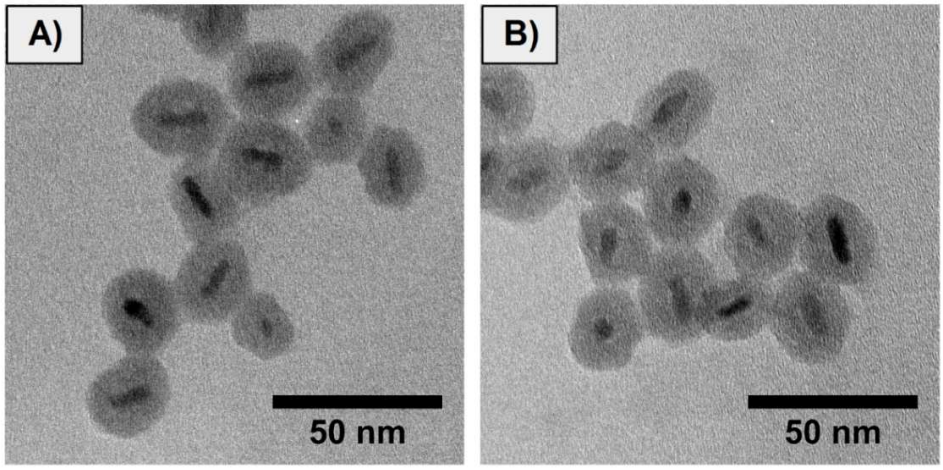

Figure S5. TEM images of a) CdSe/CdS NRs and b) CdSe/CdS/ZnS NRs encapsulated in a silica matrix which display no tip-to-tip connections. The NRs were encapsulated in a silica matrix through a water-in-oil microemulsion process according to a procedure described in the literature.[15] Briefly, 0.2 nmol of NRs was mixed to 2 mL of heptane and 640 µL of surfactant (Brij30). After 15 minutes of stirring 110 µL of 3% ammonia solution in Milli-Q water was added to the mixture. After 1 hour of stirring, 25 µL of tetraethyl orthosilicate (TEOS) was added. The reaction was stopped after 3 day by adding 2 mL of EtOH in order to destabilize the microemulsion. The nanoparticles were collected by centrifugation and purified by repeated centrifugation in EtOH and two times in Milli-Q water. The particles were stored in Milli-Q water.

Section S2:
ICP analysis: the intrinsic & molar absorption coefficient.

The intrinsic absorption coefficient, μ_i (Hens et al.[1]) is related to the absorbance, A, the volume fraction, f, and the optical length, L, of a nanocrystal (NC) dispersion.

$$\mu_i = \frac{A \ln(10)}{f L} \quad \text{Eq. S1}$$

The volume fraction of the samples can be determined as such :

$$f = \frac{Vol_{NCs,tot}}{Vol_{NCs,tot} + Vol_{solvent}} = \frac{Vol_{NCs,tot}}{Vol_{solvent}} \quad \text{Eq. S2}$$

And the total volume of NCs :

$$Vol_{NCs,tot} = \frac{N_{Cd}}{2} \; x \; Vol_{CdS\ wurtzite\ unit} + \frac{N_{Zn}}{2} \; x \; Vol_{ZnS\ wurtzite\ unit} \quad \text{Eq. S3}$$

Table S2. Overview of the ICP measurements.

Composition	Type	Volume particles (nm^3)	ICP cadmium concentration (mg/L) ± stdev	Cd (mol)	ICP zinc concentration (mg/L) ± stdev	Zn (mol)	Volume fraction (cm^{-1})
CdSe/CdS	QD	418.5	72.3 ± 0.9	7.0707E-06	-	-	0.000223342
CdSe/CdS/ZnS	QD	583.5	137 ± 2	1.34532E-05	24.4 ± 0.3	4.10352E-06	0.000526647
CdSe/CdS/CdZnS	QD	1107.0	179 ± 2	1.74912E-05	4.24 ± 0.03	7.1309E-07	0.000570167
CdSe/CdS/CdZnS/ZnS	QD	1064.7	70.4 ± 0.9	6.88425E-06	7.69 ± 0.05	1.2929E-06	0.000249495
CdSe/CdS	NR	309.1	160 ± 0.6	1.5608E-05	-	-	0.000493012
CdSe/CdS/ZnS	NR	427.6	60.6 ± 0.6	5.92859E-06	12.5 ± 0.1	2.10488E-06	0.000239433
CdSe/CdZnS	QD	876.8	518 ± 6	5.06894E-05	7.60 ± 0.05	1.27864E-06	0.001632816
CdSe/CdZnS/ZnS	QD	965.2	187 ± 2	1.83099E-05	26.7 ± 0.3	4.49622E-06	0.000689786

Figure S6 shows the intrinsic absorption coefficient obtained through ICP analysis. A decrease is observed at high energies upon ZnS shell growth consistent with the theoretical predictions (see **Section S3**).

ICP also allows us to also normalize the absorption spectra to the QD concentration. Doing so, these concentration normalized spectra actually represent the molar absorptivity ε, where the value of ε at the band gap ε_{gap} can be directly related to the (radiative) decay rate through[2]:

$$\tau^{-1} = \frac{2e}{\pi N_A \hbar c^2} n_s^2 \omega^2 \frac{\ln(10)}{g} \varepsilon_{gap} \quad \text{Eq. S4}$$

As such, a decrease in ε_{gap} can be correlated to changes in the (radiative) decay rate. We should note that this is only valid for isotropic systems (*e.g.* spherical QDs) where the absorption and emission is equal along all symmetry axes of the structure. We indeed observe simultaneous decrease in ε_{gap} and an increase in the lifetime for the spherical QDs. Taking a rod-like structure, the symmetry between absorption and emission rates breaks down as the absorption is still random along all directions (in a non-aligned, random dispersion) but the emission is affected strongly by the varying dipole moments and screening along different axes. It is beyond the scope of this work to evaluate this, but the data **in Figures 8d (inset)** and **8f** seem to suggest that this discrepancy is not trivial.

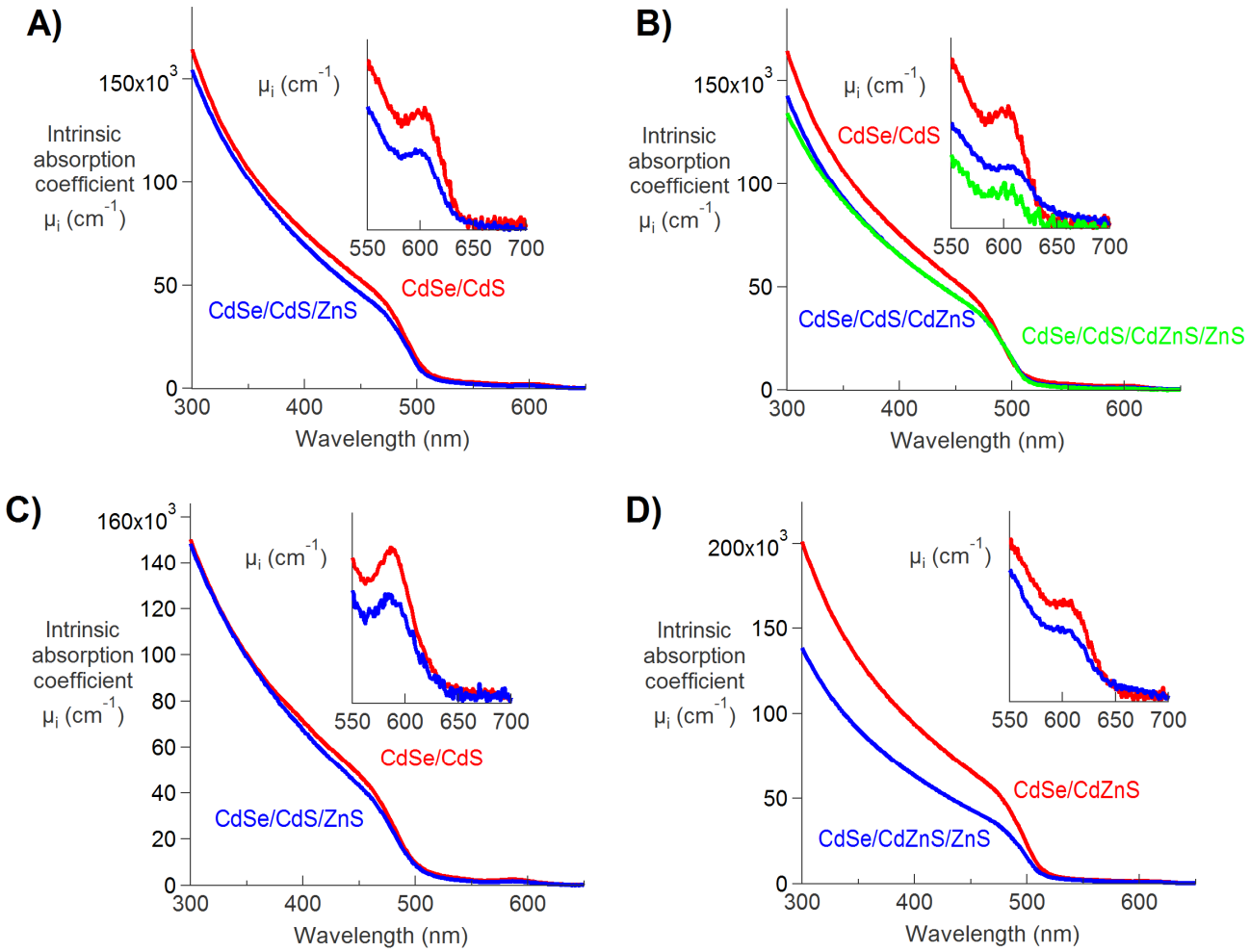

Figure S6. Intrinsic absorption coefficient spectra of (a) CdSe/CdS and CdSe/CdS/ZnS QDs (inset: focus on the excitonic feature at 600 nm), (b) CdSe/CdS/CdZnS and CdSe/CdS/CdZnS/ZnS QDs (inset: focus on the excitonic feature at 600 nm), (c) CdSe/CdS and CdSe/CdSe/ZnS NRs (inset: focus on the excitonic feature at 600 nm) and (d) CdSe/CdZnS and CdSe/CdZnS/ZnS QDs (inset: focus on the excitonic feature at 600 nm).

Section S3:
Theoretical calculation of the intrinsic absorption coefficient.

The intrinsic absorption coefficient was calculated using the procedure of De Geyter *et al*.[3] We model the system as a CdS/ZnS concentric core/shell QD and use the bulk optical constants of w-CdS and w-ZnS obtained from Adachi.[4] The approximation that the CdSe/CdS can be seen as a CdS-only system stems from the large volume fraction of the CdS shell compared to the CdSe core. We clearly observe that exchanging an amount of Cd for Zn decreases the intrinsic absorption coefficient due to a reduced absorption strength of w-ZnS compared to w-CdS along the material's c-axis. Please note that the values at 300 nm in Figure S6 are smaller compared to the theory due to the presence of a CdSe core. As such, **Figure S7** is only a qualitative description of the Zn-for-Cd effect.

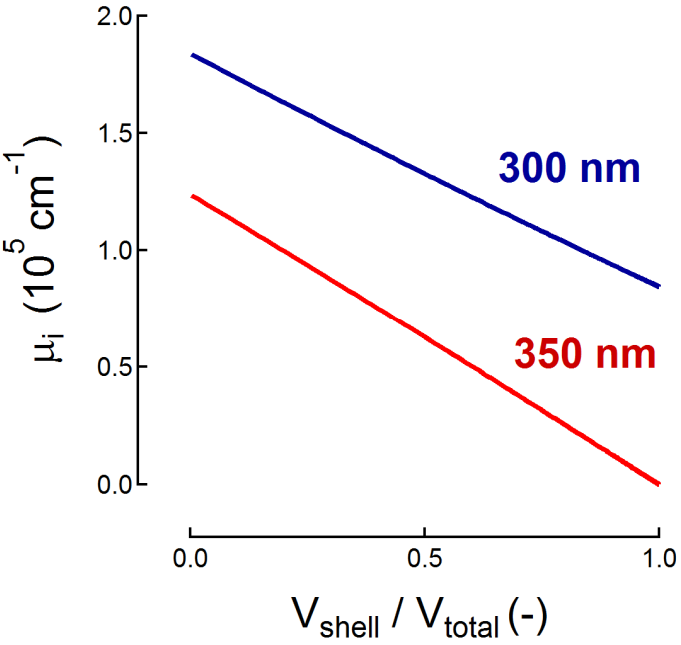

Figure S7: Intrinsic absorption coefficient of spherical CdS/ZnS core/shell quantum dots at 300 (blue) and 350 nm (red) for varying compositions going from 0 (pure CdS) to 1 (pure ZnS). The evolution shows that diluting a particle with zinc at fixed volume makes it absorb less, an observation that can be understood from the poor absorption of w-ZnS along the c-axis compared to CdS.

Section S4:
NMR spectra.

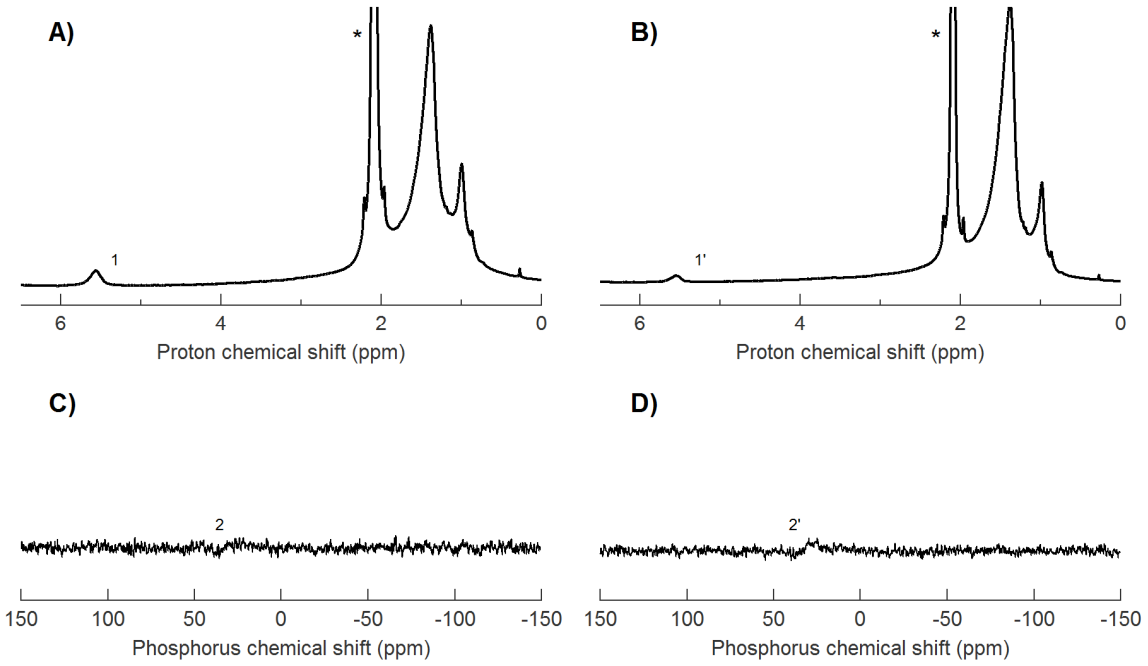

Figure S8. ^{1}H NMR spectra of CdSe/CdS/ZnS a) QDs and b) NRs. ^{31}P NMR spectra of CdSe/CdS/ZnS c) QDs and d) NRs. (1) and (1') are the alkene resonances of the zinc oleate bounded to the QDs and NRs. However, the small residual signal in the long (7000 scans) phosphorus spectra, (2) and (2'), suggests that there is still a minor fraction of cadmium phosphonate at the surface. (*) Residual toluene peak.

Section S5:
Bibliography

1. Hens, Z. & Moreels, I. Light Absorption by Colloidal Semiconductor Quantum Dots. *J. Mater. Chem.* **22,** 10406–10415 (2012).

2. Moreels, I. *et al*. Size-dependent optical properties of colloidal PbS quantum dots. *ACS Nano* **3,** 3023–30 (2009).

3. De Geyter, B. & Hens, Z. The absorption coefficient of PbSe/CdSe core/shell colloidal quantum dots. *Appl. Phys. Lett.* **97,** (2010).

4. Adachi, S. *Optical Constants of Crystalline and Amorphous Semiconductors*. (Kluwer Academic, 1999).